A Controlled CO_2 Release Experiment in a Fault Zone at the In-Situ Laboratory in Western Australia

Karsten Michael[1], Arsham Avijegon[2], Ludovic Ricard[1], Matt Myers[1], Konstantin Tertyshnikov[3], Roman Pevzner[3], Julian Strand[1], Allison Hortle[1], Linda Stalker[1], Marina Pervukhina[1], Brett Harris[3], Andrew Feitz[4], Bobby Pejcic[1], Alf Larcher[1], Praveen Rachakonda[1], Barry Freifeld[5], Mark Woitt[5], Laurent Langhi[1], Tess Dance[1], Jo Myers[6], Jennifer Roberts[7], Erdinc Saygin[1], Cameron White[1], Mojtaba Seyyedi[1]*

[1]CSIRO Energy, 26 Dick Perry Ave, Kensington 6151 WA, Australia
[2]GASS Petroleum Pty Ltd, Perth, WA, Australia
[3]Curtin University, Perth, WA, Australia
[4]Geoscience Australia, Canberra, Australia
[5]Class VI Solutions Inc., Oakland, United States of America
[6]CSIRO Oceans & Atmosphere, Perth, WA, Australia
[7]Strathclyde University, Glasgow, United Kingdom

**Corresponding author: karsten.michael@csiro.au, ph: +61 8 6436 8759*

Abstract

A controlled-release test at the In-Situ Laboratory Project in Western Australia injected 38 tonnes of gaseous CO_2 between 336-342 m depth in a fault zone, and the gas was monitored by a wide range of downhole and surface monitoring technologies. Injection of CO_2 at this depth fills the gap between shallow release (<25 m) and storage (>600 m) field trials. The main objectives of the controlled-release test were to assess the monitorability of shallow CO_2 accumulations, and to investigate the impacts of a fault zone on CO_2 migration.

CO_2 arrival was detected by distributed temperature sensing at the monitoring well (7 m away) after approximately 1.5 days and an injection volume of 5 tonnes. The CO_2 plume was detected also by borehole seismic and electric resistivity imaging. The detection of significantly less than 38 tonnes of CO_2 in the shallow subsurface demonstrates rapid and sensitive monitorability of potential leaks in the overburden of a commercial-scale storage project, prior to reaching shallow groundwater, soil zones or the atmosphere.

Observations suggest that the fault zone did not alter the CO_2 migration along bedding at the scale and depth of the test. Contrary to model predictions, no vertical CO_2 migration was detected beyond the perforated injection interval. CO_2 and formation water escaped to the surface through the monitoring well at the end of the experiment due to unexpected damage to the well's fibreglass casing. The well was successfully remediated without impact to the environment and the site is ready for future experiments.

Key words: CO_2 controlled-release; Western Australia, CO_2 geological storage; fault zone; CO_2 monitoring

1. Introduction

Although adequate site selection and characterisation of a CO_2 storage project will make leakage of CO_2 and migration to the shallow environment unlikely, storage project operators may need to provide adequate monitoring systems for assuring regulators and the public that leakage could be confidently detected, managed and remediated. One of the challenges is the timely identification of leakage, i.e. the ability to detect small volumes of CO_2 as early as possible on its migration path between the storage complex and groundwater resources or the atmosphere (Jenkins et al., 2015). Therefore, monitoring technologies need to be employed that are cost effective and have adequate depth, temporal and spatial coverage.

Previous field tests have focussed on shallow-release experiments performed at less than 25 m depth (Roberts and Stalker, 2017; Roberts et al., 2018) or CO_2 storage experiments at more than 600 m depth (Michael et al., 2010 and references therein). However, except for a few recent projects in Canada (Macquet and Lawton, 2019) and eastern Australia (Feitz et al., 2018), experiments investigating the migration behaviour and detectability of gaseous CO_2 at intermediate depths between 25 m and 600 m have been lacking. More information for this depth interval would be helpful for improving monitoring schemes of large-scale CO_2 storage projects by demonstrating detectability of CO_2 leakage before it reaches potable groundwater or the atmosphere.

Furthermore, the identification and characterisation of potential leakage processes and pathways are important for developing properly targeted monitoring schemes (Birkholzer et al., 2014, Michael et al., 2016). For example, fault zones have been identified as a potential leakage pathway that may concentrate or focus CO_2 migration upward to the shallow subsurface, potentially accumulating in groundwater aquifers or continuing to migrate to the atmosphere (e.g. IPCC, 2005; Lewicki et al., 2007; Kaldi et al., 2013). Leakage from natural analogue CO_2 stores occurs along faults (e.g. Miocic et al., 2016, Roberts et al., 2019 and references therein). Studies of these natural analogues find that faults are complex and channel fluids heterogeneously at depth and towards the surface (Roberts et al., 2015) and so understanding of how faults might affect CO_2 leakage is poorly constrained.

The CSIRO In-Situ Laboratory Project (In-Situ Lab) is located at the eastern edge of the South West Hub CCS Flagship project (SW Hub) in Western Australia (Figure 1), which has been identified as a potential area for commercial-scale CO_2 storage (Stalker et al., 2013). The storage concept of the SW Hub involves injection of CO_2 into a more than 2000 m deep, 1000 m thick sandstone reservoir, the Wonnerup Member of the Lesueur Sandstone, where up to 800,000 t CO_2/year over 30 years are predicted to be potentially contained, largely due to residual trapping and dissolution of CO_2 in formation water (Sharma and Van Gent, 2019). Given the faulted nature of the storage complex and lack of a conventional seal, it is important to understand the CO_2 migration along faults and the ability to identify and monitor potential leakage pathways for assurance purposes.

The In-Situ Lab addresses the two general science gaps related to monitoring leaks from a CO_2 storage complex outlined above. It consists of two wells at approximately 400 m depth drilled into a major fault zone (F10 Fault), which allows performing controlled-release experiments that can reduce uncertainty regarding: 1) the monitorability of shallow, gaseous CO_2 accumulations that may result from leakage from a storage complex, and 2) two-phase flow processes in a fault zone. The project contributes to broadening the global portfolio of controlled CO_2 release tests, with the aim to increase regulators' and the public's confidence in storage safety, and in the protection of groundwater resources and the environment.

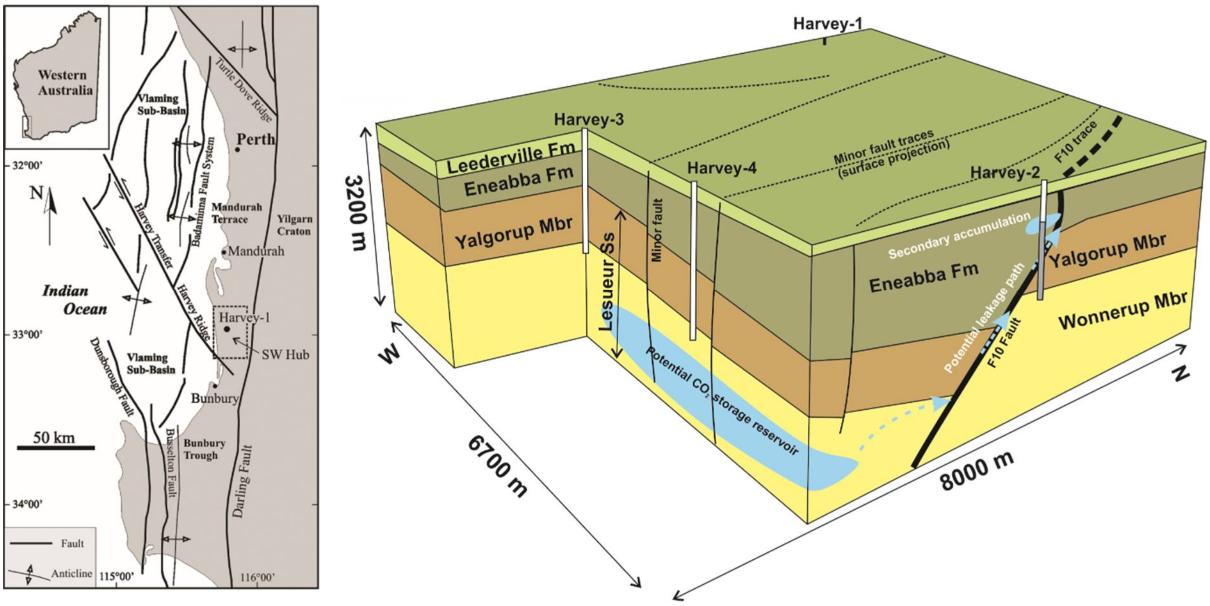

Figure 1. Location of the existing well locations within the proposed greater storage complex. Harvey 2 was drilled in the east of the study area, where major displacement along the F10 fault forms the eastern boundary to the storage complex. Harvey 2 was backfilled with cement (grey shading) up to a depth of approximately 400 m.

1.1 Geological setting

Previous seismic surveys and analyses of data from four wells (Harvey-1, -2, -3 and -4) drilled for the SW Hub project between 2011 and 2015 (Stelfox, 2017) were supported by a series of research projects (Stalker et al., 2014; Stalker and Van Gent, 2018) and new data from the ISL OB-1 well to provide more detail on the geology of the In-Situ Lab. Harvey-2 was drilled by the SW Hub in the vicinity of the large F10 fault as a data well for the geological characterisation beyond eastern edge of the storage complex.

The In-Situ Lab is centred around Harvey-2, which was intended to be recompleted as an injection well. It is situated on a north-west trending broad basement high within the Southern Perth Basin. Faulting is attributed to normal and strike-slip deformation of the Phanerozoic sedimentary cover (Crostella and Backhouse, 2000). The Mesozoic sequence at the In-Situ Lab site comprises Triassic and Jurassic sediments below a significant Early Cretaceous unconformity, overlain by later Cretaceous to recent deposits (Figure 2a). The Middle to Late Triassic Lesueur Sandstone (composed of the lower Wonnerup and upper Yalgorup members) and the Eneabba Formation, the injection interval, consist of fluvial to shallow marine siliciclastic units in the southern part of the Perth Basin (Playford et al., 1976; Mory, 1995; Olierook et al., 2014). Palynology indicates that the base of the Eneabba Formation is intersected in Harvey-2 somewhere between 610 and 730 m, though similarity between the sediments of the Eneabba Formation and the Yalgorup Member and tectonic disruption make more precise definition difficult.

Major fault reactivation, block rotation, uplift and erosion occurred across the Perth Basin during the Valanginian (~135 Ma) (Crostella and Backhouse, 2000; Bradshaw et al., 2003). At the In-Situ Lab, the unconformity currently lies at ~200 m below surface (Rockwater, 2015). Above the unconformity the Leederville Formation contains up to 100 m of horizontally bedded, Late Valanginian to Aptian, poorly consolidated, clastics, shales and lignite seams (Playford et al., 1976). The Pleistocene Guildford Formation lies below surficial sediments and disconformably on Leederville Formation strata comprising alluvial sand and clay with shallow-marine and estuarine lenses, with a basal conglomerate (Low, 1971).

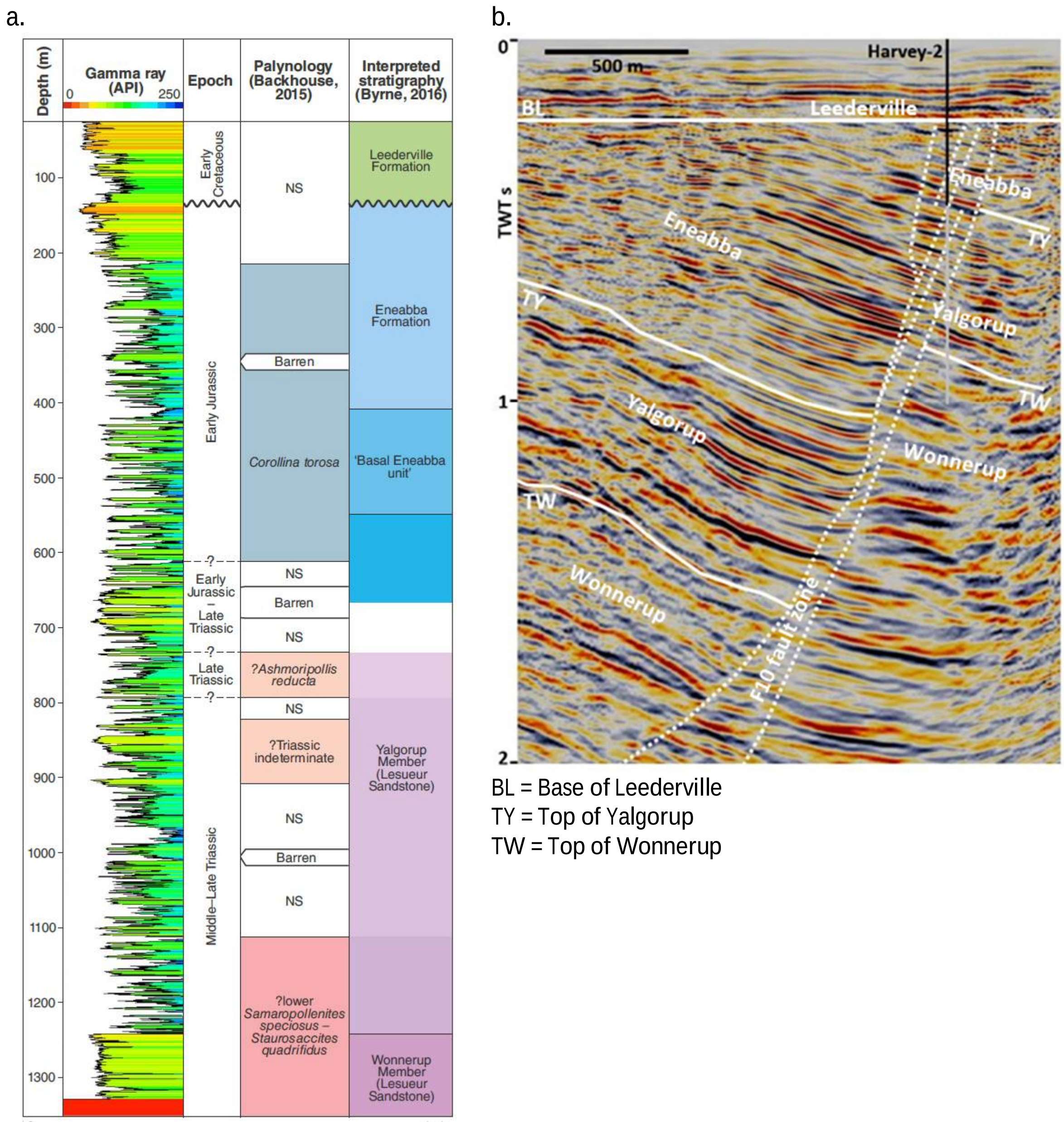

Figure 2. Geology at the In-Situ Lab site: a. Gamma ray log, palynology and stratigraphy in Harvey-2 (Stelfox, 2017), and b. W-E seismic cross-section through Harvey-2 and across the F10 fault (vertical scale in two-way-time).

The Eneabba Formation, the injection target, is interpreted to be a Jurassic continuation of the predominantly fluvial-alluvial to perhaps fluvio-deltaic environment of the Late Triassic Yalgorup Member (Timms et al., 2015). Previous analyses of cores from wells in the area have demonstrated that the Yalgorup Member is highly heterogeneous and consists of a lithofacies that can be ascribed mainly to fluvial moderate to high energy river channels and low energy floodplain settings, including paleosols (Timms et al., 2012; Delle Piane et al., 2013; Olierook et al., 2014; Lim et al., 2017). Formation Micro-imager (FMI) analysis on the nearby Harvey-4 well, integrated with the natural gamma ray spectroscopy (NGS) tool and bedding dip measurements data have been interpreted into depositional environments such as braided bar, point bar, splays, overbank and paleosols, other descriptive interpretation included evaporitic shale and siderite cementation (Roestenburg, 2016). The result is an interlayered system of low- to high-permeability sandstones and low-permeability siltstones and paleosols. The Yalgorup Member and the Eneabba Formation contain lithology with highly variable porosity and permeability (Figure 3).

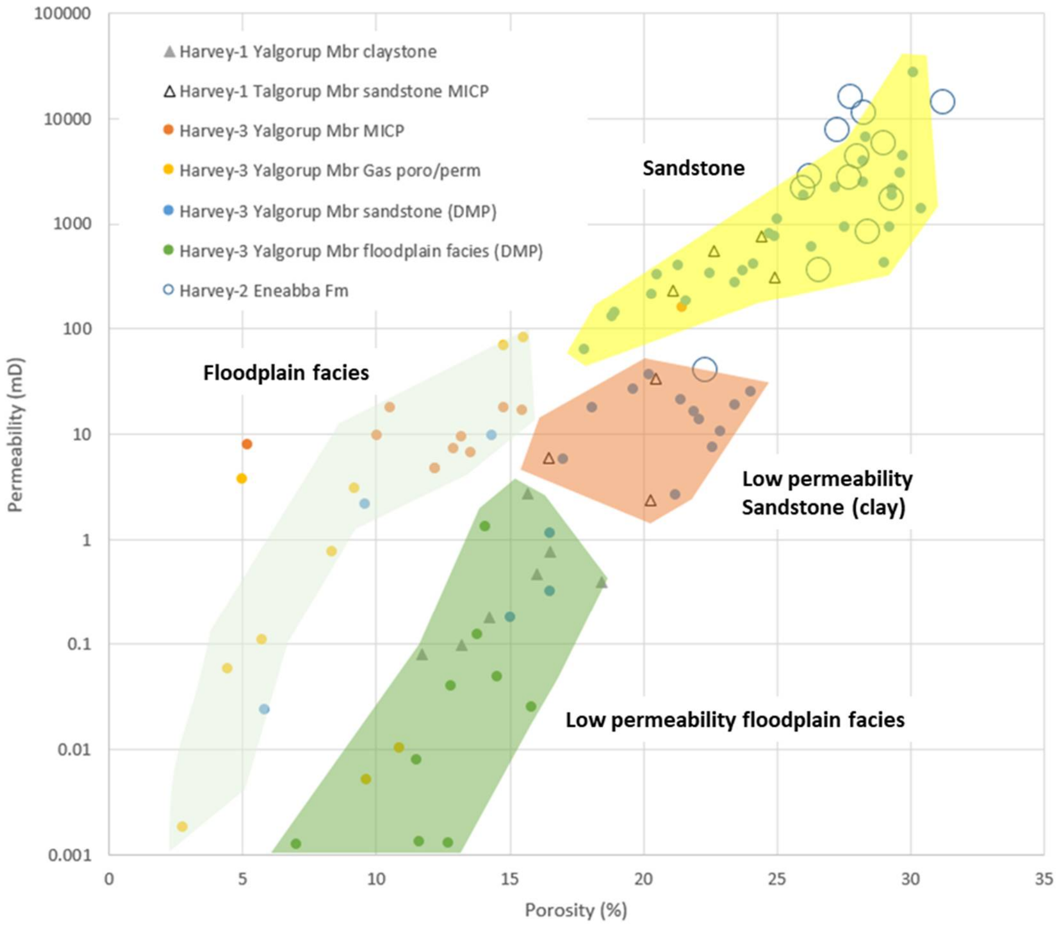

Figure 3. Porosity versus permeability core analysis data for the Yalgorup Member (modified from Bourdet et al., 2019) compared to newly measured data from the Eneabba Formation (hollow circles). DMP identifies data provided by the Western Australian Department of Mines and Petroleum, which was renamed Department of Mines, Industry Regulations and Safety (DMIRS).

As part of the In-situ Lab Project core analyses of the Eneabba Formation from the Harvey-2 drill hole were undertaken. Air permeability was determined with a Hassler flow cell. The resulting porosity-permeability values are notably high, with a mean exceeding 5 D and 28 % porosity for the sands (Figure 3). Unsteady-state CO_2-brine relative permeability analyses were performed for five samples in the injection interval.

1.2 Structural characterisation and local stress regime

The main structural feature in the project area is the F10 fault zone. It divides two structural blocks with Harvey-2 penetrating through F10 into the footwall block (Figure 2b) and the other Harvey wells to the west penetrating the hanging wall block (Figure 1). The faults in the Mesozoic sedimentary succession are truncated by the Early Cretaceous unconformity. The main F10 fault displacement is 1600 m at the top Sabina Sandstone, 1000 m at the top Wonnerup Member and 750 m at the top of the Yalgorup Member. Fault movement is interpreted on seismic reflection data as mostly normal. The faults have typical normal fault dips of around 60° to 70°.

Approximately 225 m of disaggregation have been interpreted in the ~650 m F10 fault zone intersection in Harvey-2. Disaggregation occurs between lenses of less deformed lithology, including intersections of apparently undeformed sediments. The disaggregated units tend to be sandstones; adjacent oxidised hardpans, silty paleosols and silts are more competent at the time of deformation. Once reconstructed, the true thickness of the fault zone in F10 is 200 to 300m, which, based on published data, is typical for a fault of the magnitude of F10 (Childs et al., 2009). Within the reconstructed fault zone there is approximately 70 to 100 m thickness of disaggregated fault rock, constituting a quarter to a third of the fault zone thickness. The thickness of disaggregated fault rock would be towards the upper end of the range extrapolated from compiled published fault data (Childs et al., 2009). This is potentially due to low effective stress conditions present during shallow faulting.

The occurrence of disaggregation as the dominant faulting mechanism, typical of shallow faulting at depths less than 1 km (Fulljames et al., 1997; Sperrevik et al., 2002; Bense et al., 2013) in Harvey-2 at 849 m depth suggests that, at the In-Situ Lab site, a maximum of not much more than 300 m of Jurassic sediments would have been eroded for the burial depth at the time of faulting to be in the vicinity of ~1000 m.

Based on the limited data and previous studies available for the area, the in-situ stress regime at shallow depth in Harvey-2 is a strike-slip fault regime with the major horizontal stress slightly above or equal to the vertical stress. King et al. (2008) determined the vertical, minimum and maximum horizontal stress gradients in the Northern Perth Basin at 400 m depth to be 21.6 kPa/m, 18.5 kPa/m and 21.7 kPa/m, respectively. Slip tendency analysis (Morris et al., 1996; Lisle and Srivastava, 2004) was carried out on all the seismically mapped SW Hub faults, however given the orientation of the principal stress (105^{o}) in the strike-slip regime and the dominantly N-S orientation of the faults none of the faults in the area are predicted to be close to reactivation (Langhi et al., 2013). In other words, under increasing pressures, new faults would form in the direction of and constrained by the minimum horizontal stress before reactivation of existing faults.

Rock mechanical tests were conducted on several core plugs obtained from the injection zone in Harvey-2. The core materials were extremely weak, and the test plugs had to be frozen during the sample preparation and experimental set up. The stress-strain curves for the two triaxial tests show a highly ductile/strain hardening plastic deformation behaviour. As such, no distinctive peak strength could be identified from the stress-strain curves.

2. Test design

The In-situ Lab project commenced in May 2018 with the concept of developing an enduring test site for controlled CO_2 release experiments in a shallow fault zone by the end of May 2019.

2.1 Concept

A controlled CO_2 release test to mimic a shallow CO_2 accumulation in the vicinity of a fault zone was designed and conducted for:

1. Demonstrating the detection and monitorability of shallow gaseous CO_2 accumulations by testing a comprehensive range of monitoring technologies, and
2. Investigating the impact of faults and fault zone geometry on two-phase leakage processes by injecting CO_2 into a faulted interval in the Eneabba Formation and monitoring the plume behavior.

To achieve these objectives, the In-Situ Lab: 1) recompleted the existing Harvey-2 – primarily for CO_2 injection; 2) drilled and completed a fibreglass geophysical monitoring well ISL OB-1, with behind-casing instrumentation, and 3) drilled and completed a groundwater well in the Surficial aquifer (Figure 4). It should be noted that the focus of the experiment was the monitorability of a CO_2 plume in the shallow subsurface. In this context, the purpose of CO_2 injection was to mimic leakage from a deeper reservoir and secondary accumulation along the leakage path. Therefore, the assessment of induced seismicity or potential fault reactivation, like for example in experiments by Guglielmi et al. (2015), were outside the project scope.

A range of surface and borehole geophysical technologies were deployed to monitor the plume of injected CO_2. Groundwater and soil gas sampling were undertaken for assurance monitoring purposes to detect any vertical CO_2 migration to the overlying shallow aquifer or the atmosphere.

The project planned to inject up to 40 tonnes of CO_2 over 4 days based on operational considerations, including the cost and transport of CO_2 to the site, the time available for drilling and completion of the wells, as well as for conducting the injection experiment and performing associated monitoring activities.

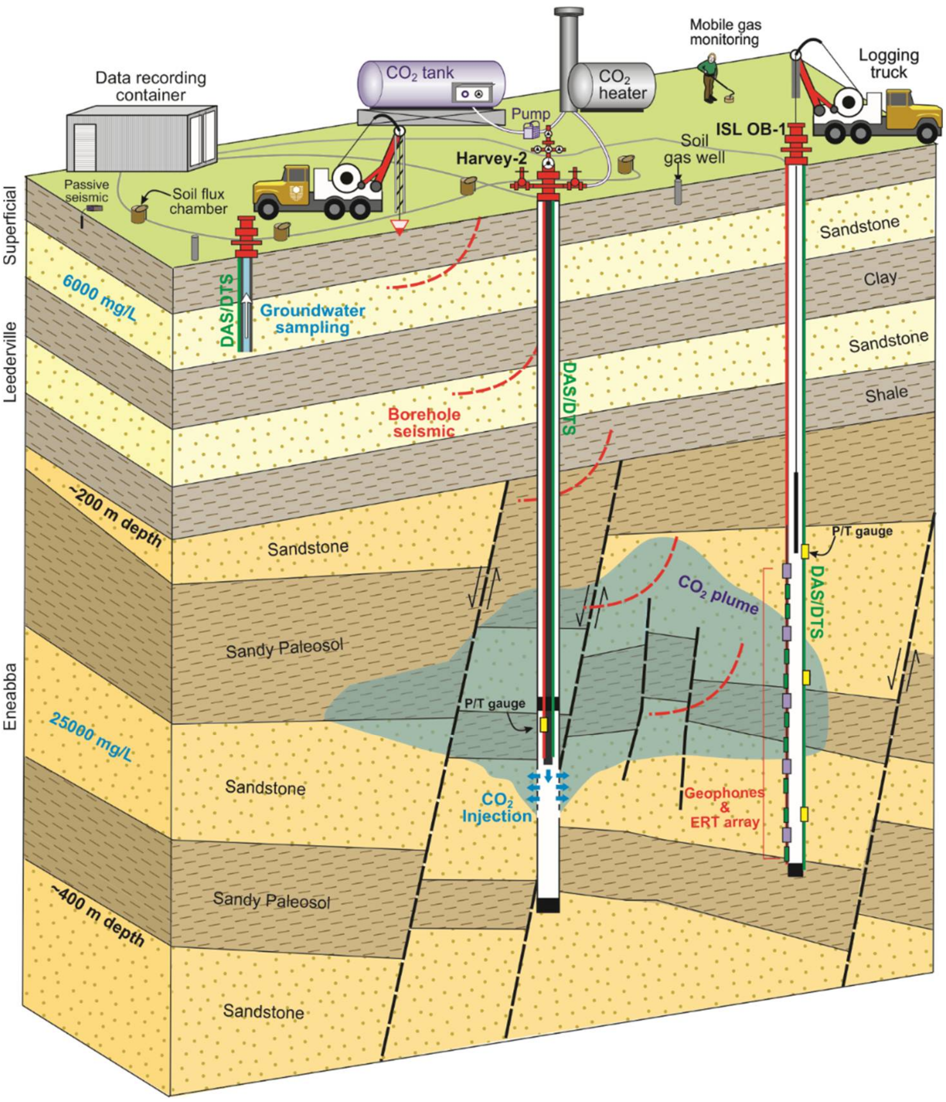

Figure 4. Schematic of the In-Situ Lab well configuration, experimental set up and monitoring activities (not to scale).

From core observations, an 11 m thick sandstone layer, overlain by a 3 m paleosol, was selected as injection interval in Harvey-2 and was perforated in the upper 6 m between 336 and 342 m depth. Due to the resolution of the existing seismic and limited well data, large uncertainty existed regarding the detailed fault zone geometry, and, more specifically, how disaggregation and drag has impacted the contiguity and slope of lithostratigraphic layers within the fault zone. While core intersections with visibly disrupted lithology are observed, it is not known whether fault displacements in the vicinity of the release are significant, tens to hundreds of meters potentially, or minor, on the order of a few meters or less. In other words, it was not clear to what extent the relatively low-permeability paleosols would form baffles to the migration of CO_2. Also, it was not known whether sub-seismic faults, if present, would act as horizontal flow barriers or vertical conduits to CO_2 migration.

A series of geological models was created to test the unknown fault geometry and properties. Three background lithology permeability scenarios were based on previously tested SW Hub core samples (Figure 3), three fault displacement and location scenarios and two fault permeability scenarios were combined to produce 18 models for simulation.

A numerical simulation study was undertaken to inform the optimal location for ISL OB-1 and the vertical location of the downhole instrumentation, and to ensure breakthrough of CO_2 occurred within the project timeframe for the test specific CO_2 injection rates and volume.

The 18 geological model scenarios covering different ranges of permeability configurations for the selected interval and a total injection of 40 tonnes, the extents of CO_2 saturation were computed (Figure 5). All models are based on gamma log correlations and core descriptions from Harvey-2. The range of potential degrees of faulting was represented by varying permeability configurations to reflect different degrees of continuity and structural tilt of the interlayered sandstones and paleosols (Figure 4 and b). By the end of CO_2 injection, the most likely distribution of any plume (depicted by yellow colour) would be within 10 m around the well, and over the course of the experiment it was predicted to move upwards to at least 325 m depth.

Based on the likely extent of the CO_2 plume for an injection volume of 40 tonnes, the observation well ISL OB-1 was located at 7 m from the injection well to maximise the likelihood the CO_2 plume would be intersected. The CO_2 plume was predicted to migrate vertically for at least 20 m above the injection interval into the paleosol section; hence instrumentation locations and spacings were planned accordingly.

Injectivity estimates based on the geological model and reservoir simulations confirmed that an average injection rate of 0.4 tonnes/hour and a maximum rate of 1 tonne/hour would be achievable. Reservoir pressures were predicted to stay below 4000 kPa and well below fracture pressure. No fracture testing had been performed at the site, and the fracture pressure was estimated from the regional minimum horizontal stress gradient to be approximately 6216 kPa at the top of the injection interval at 336 m depth.

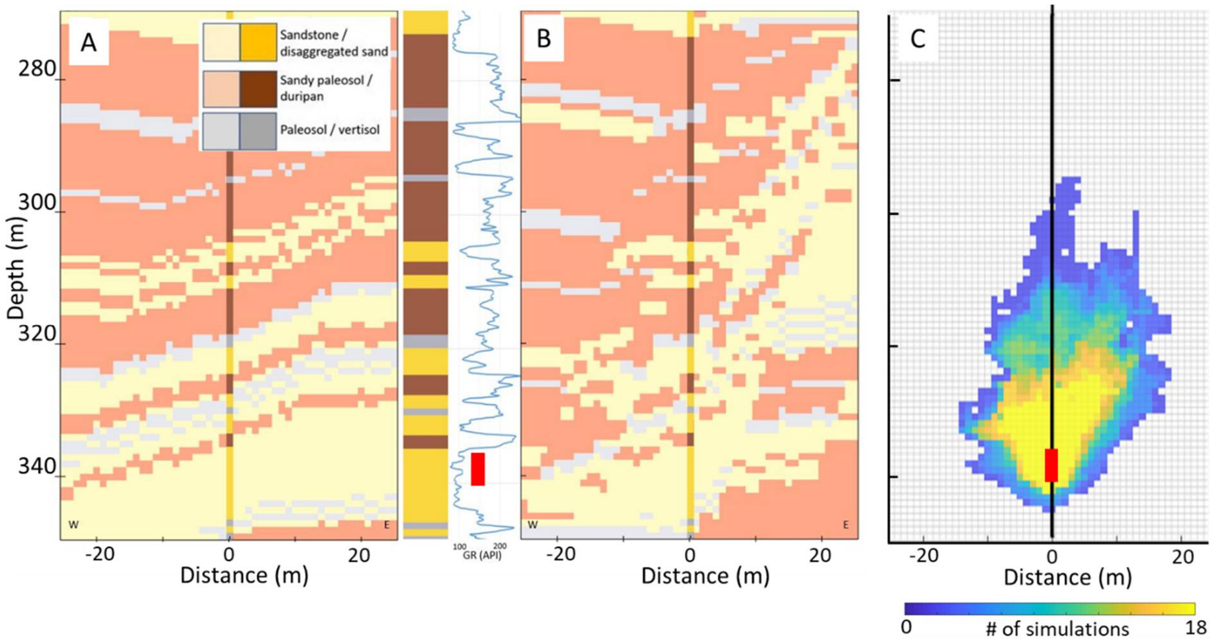

Figure 5. East-west model cross-sections showing two end members of fault zone interpretation correlated with the gamma ray log in and above the injection interval in Harvey-2: A) layered, slightly tilted and B) disturbed layering and drag in faulting direction. C) Likely CO_2 plume distributions after 40 tonnes of injection based on 18 reservoir simulations. The colour scheme reflects the number of model scenarios that predict the presences of CO_2 in each cell. The injection interval is depicted by the red bar between 336 and 342 metres depth.

2.2 Project timeline

Due to a number of constraints the project had to be delivered within a strict timeframe between May 2018 and May 2019. For Harvey-2 and ISL OB-1, completion designs were developed that formed the basis for extensive contracting and procurement activities. Permits were obtained for drilling and injection activities by October 2018.

Site preparation and field deployment commenced in November 2018. Drilling and completion of ISL OB-1 and the shallow groundwater well, re-completion of Harvey-2, mobilising equipment on site, and baseline monitoring all took place in the weeks leading up to the injection test in February 2019.

CO_2 injection was conducted in February 2019 when 38 tonnes of food-grade CO_2 were injected into Harvey-2 over a 4-day period. This was complemented by extensive subsurface and surface monitoring activities. While some monitoring activities have been continuing, CO_2 injection facilities were moved offsite, and Harvey-2 and ISL OB-1 were flushed with inhibited brine, leaving the In-Situ Lab field site ready for future experiments.

3. Experimental set up

The project footprint area is approximately 80 metres by 80 metres and centred around Harvey-2.. The surface infrastructure, including CO_2 injection facilities, was installed on a prepared surface of limestone to absorb spills and provide a uniform surface (Figure 6). The average depth of the limestone pad was 30 cm. An on-site tank was installed to store up to 300 m^3 of formation water and other wellbore fluids that were produced during well drilling and testing.

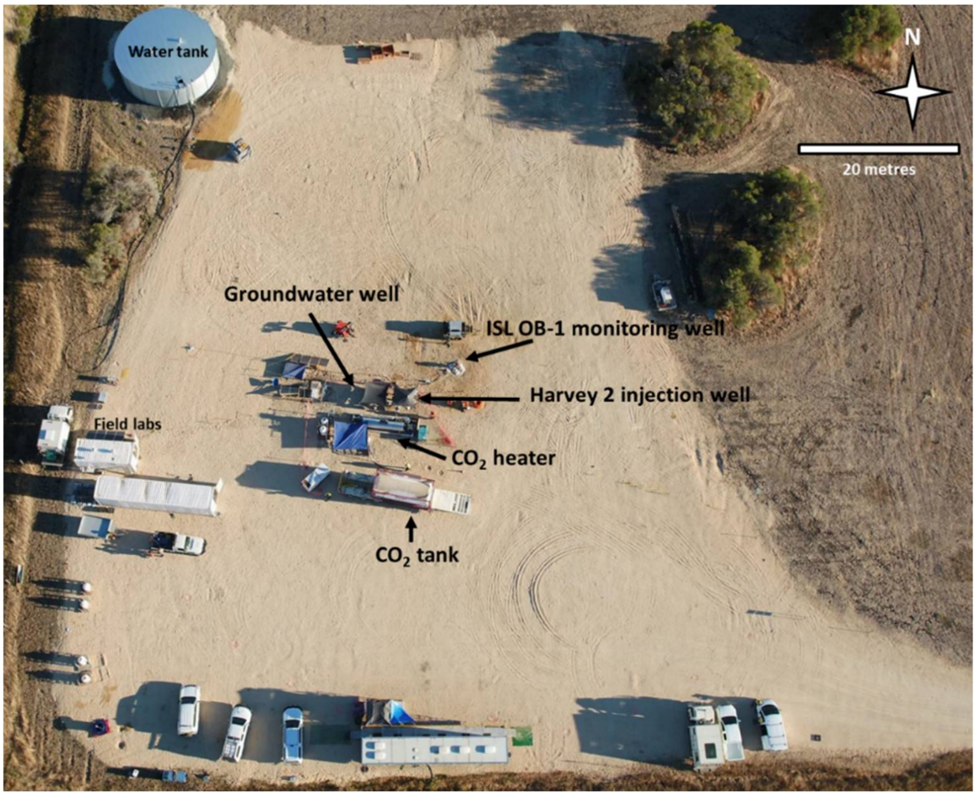

Figure 6. Aerial photo of the In-Situ Lab field site during CO_2 controlled-release experiment.

3.1 Completion and instrumentation of wells

The Harvey-2 well was perforated from 336 m to 342 m depth and an air-lift water production test resulted in an initial average flow rate of 9 L/min. Injection tubing with fibre optic cable for distributed temperature sensing (DTS) and distributed acoustic sensing (DAS), and a pressure/temperature (P/T) gauge was run into the well. An inflatable packer was installed above the perforations.

The ISL OB-1 monitoring well was drilled with a water-based mud to 378 m depth, approximately 7 m to the northeast of Harvey-2. The well encountered some borehole stability issues in the Eneabba Formation identified as breakouts in the caliper log (Figure 7). Open-hole logging was conducted (gamma ray, resistivity, density, neutron porosity, sonic and borehole magnetic resonance) prior to completion activities. Individual sandstone intervals can be correlated at similar depths in Harvey-2 and ISL OB-1 according to the gamma ray responses (Figure 7), showing no obvious vertical structural displacement between the two wells.

The ISL OB-1 well was completed with fibreglass casing and behind-casing monitoring equipment including 4 lines: a) 8 level geophone system with 3C GS-32CT 10 Hz phones at 10 m spacing; b) Electrical resistivity tomography array with 32 S/S take-outs at 3 m spacing; c) TEC line with three piezo pressure & temperature gauges; and d) Dual mode fibre optics for DAS and DTS.

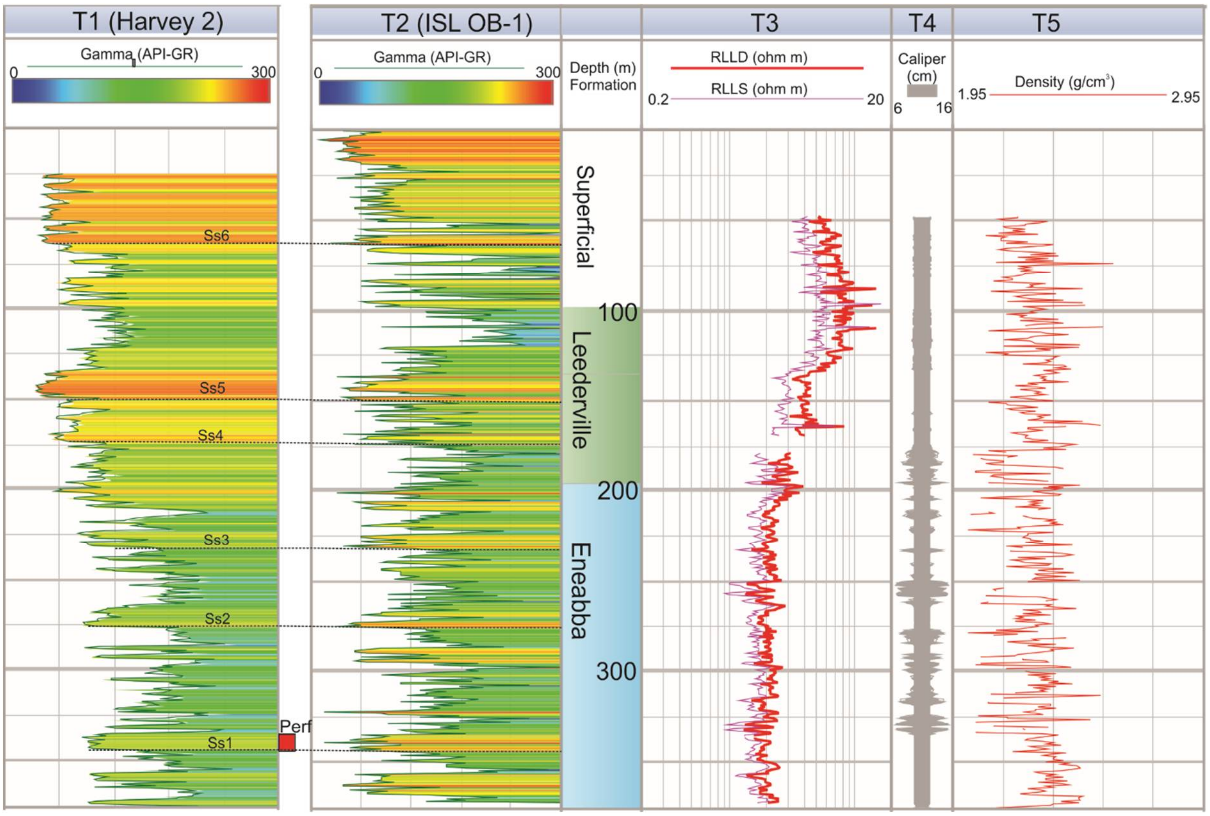

Figure 7. Selected open-hole log data. Natural radioactivity (GR) log data from Harvey-2 (T1) and log data from ISL OB-1 well (T2-T5): Gamma ray (T2), deep (RLLD) and shallow (RLLS) resistivity (T3), caliper (T4) and density (T5). Correlations between the base of selected sandstone units (Ss1-Ss6) and depicted by dashed lines between T1 and T2. The location of the perforation interval in Harvey-2 is denoted by the red box and coincides with Ss1.

Unfortunately, the wiper plug failed during the cementing of the casing before the cement fully cured, allowing the cement slurry to move back into the well to a depth of approximately 285 m. After considering the risks and various options, a decision was made to slowly drill out the cement inside the casing and logging accessibility down to 350 m was restored. Some small pieces of fibreglass were recovered in the drilling mud, suggesting that the reaming out process caused some damage to the internal lining of the casing. The well was inspected with a camera during the reaming, but only minor damage was noted.

Towards the end of the cementing activity, the three pressure and temperature gauges in ISL OB-1 failed, most likely due to increased temperatures and strain during cement curing.

A PVC cased shallow monitoring well was drilled to a depth of 27 m and instrumented with a fibreoptic cable outside the casing and a P/T gauge to provide continuous monitoring and groundwater sampling throughout the project.

3.2 Surface injection system

The surface injection system consisted of an ISO tank to supply liquid CO_2, a pump to maintain the CO_2 in the liquid phase and provide sufficient pressure for injection; followed by a heater to vaporise the pressurised CO_2 prior to entering the well (Figure 8).

The ISO tank contained food-grade gas supplied from BOC with a nominal pressure between 2000 and 2400 kPa. At 2400 kPa the vapour/liquid equilibrium temperature is approximately -13 °C. The tank was refilled twice by tanker truck.

An air-compressor powered AGD-7 gas pump from Haskell which can handle both liquid and vapour CO_2 was initially chosen based on piston volume and pressure rating. This pump ended up not achieving the required pump rates and, after first combining it with an ASF-B10 liquid pump, was later replaced by a larger ATV-8 liquid pump (Figure 8).

As the initial reservoir conditions (T = 31 ^{o}C and p = 3300 kPa) were subcritical with CO_2 existing within the gas phase, a propane-fired atmospheric water bath heater exchange with a rating of 750000 Btu/hr was used for vaporization. The enthalpy difference at 2400 kPa between -18 °C liquid and 30 °C vapour is 265000 Btu/kg. At 0.8 tonnes per hour of CO_2, this corresponds to 212000 Btu/hr of heating.

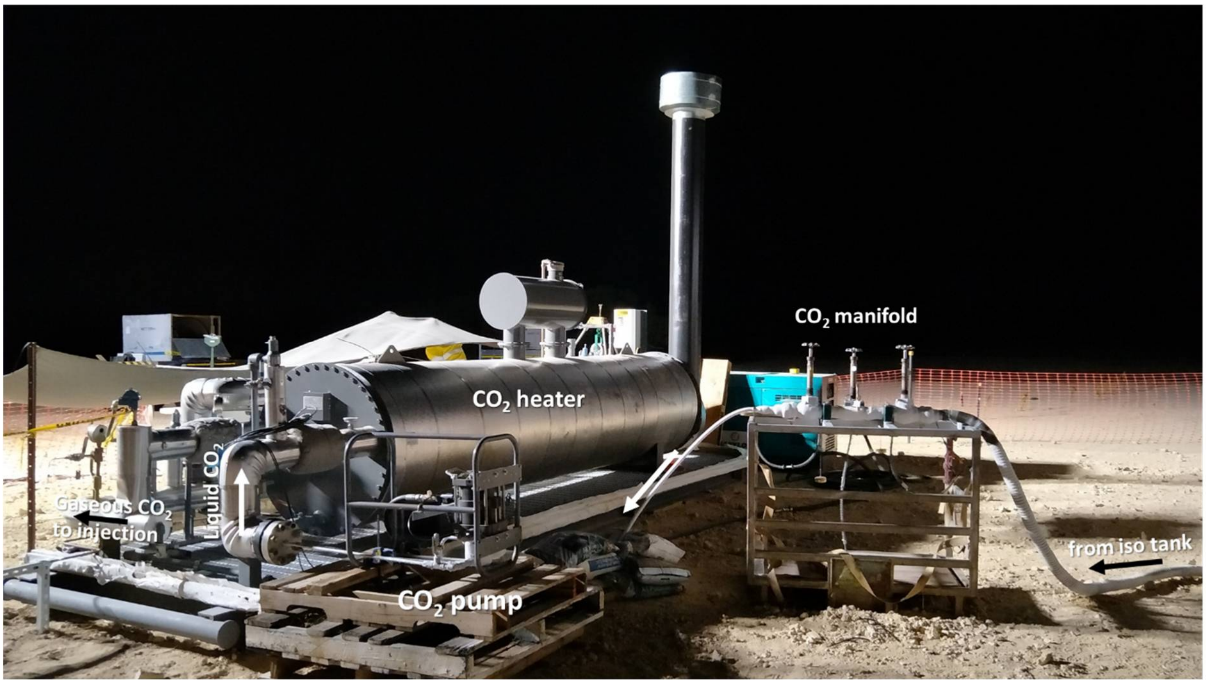

Figure 8. Photograph showing the surface infrastructure and delivery pathway of the CO_2 injection system.

3.3 Monitoring scheme

Monitoring activities during the controlled-release experiment included: 1. Pressure and temperature monitoring for real-time management of the injection operation; 2. Borehole geophysics, fibre optic sensing and logging for detection and spatial delineation of the CO_2 plume; and 3. Near surface assurance monitoring, including passive seismic, atmospheric, soil gas concentration and flux measurements, as well as groundwater sampling to detect any impacts from the operational activities or any anomalous CO_2 from the injection experiment at the surface (Figure 4).

Pressure and temperature monitoring

During the test, wellhead pressure, temperature at various points in the injection line and ISO tank pressures were recorded and used to calculate CO_2 injection rates. Pressure and temperature were continuously monitored with the p/T gauge in Harvey-2 to ensure the appropriate conditions for injection of gaseous CO_2. DTS measurements were taken continuously pre-, during and post-injection in Harvey-2, ISL OB-1 and the groundwater well.

Borehole seismic

The seismic monitoring program was focused on the borehole approach as it is well recognised for the time-lapse observations of a reservoir providing great repeatability (Pevzner et al., 2010; Tertyshnikov et al., 2017; Tertyshnikov et al., 2018). It allows for comparatively fast acquisitions for the repeated surveys and has limited land access issues. The monitoring surveys and a characterisation survey took place from 31st of January to 19th of February 2019. Both project wells (Harvey-2 and ISL OB-1) were instrumented with fibre optic cables. In Harvey-2 the cable was deployed on production tubing. In ISL OB-1 a hybrid cable containing fibre optics and eight three component geophones, was cemented behind the casing. The single mode cores of these cables were utilised for the distributed acoustic sensing (DAS).

Several borehole seismic techniques were applied and trialled during the experiment. The offset vertical seismic profiling (VSP) monitoring acquisitions were set up as a series of lines extended from around the ISL OB-1 well within the north-eastern quadrant (due to the permitted land access) and spaced every ten degrees (Figure 9). A low power light seismic source (a 45 kg accelerated weight drop) was used for the surveys. The source delivered sufficient energy and frequency content (examples of raw shots are shown in Figure 9) for the shallow depths of investigation and satisfied the low-invasiveness requirements for the farmlands. In total, nine surveys were acquired including the initial baseline dataset. Eight excitations per shot point were performed to increase the signal to noise ratio. The recording parameters for the DAS acquisition were a pulse repetition frequency of 50 kHz, 2 seconds record length, and a channel step of 0.5 m.

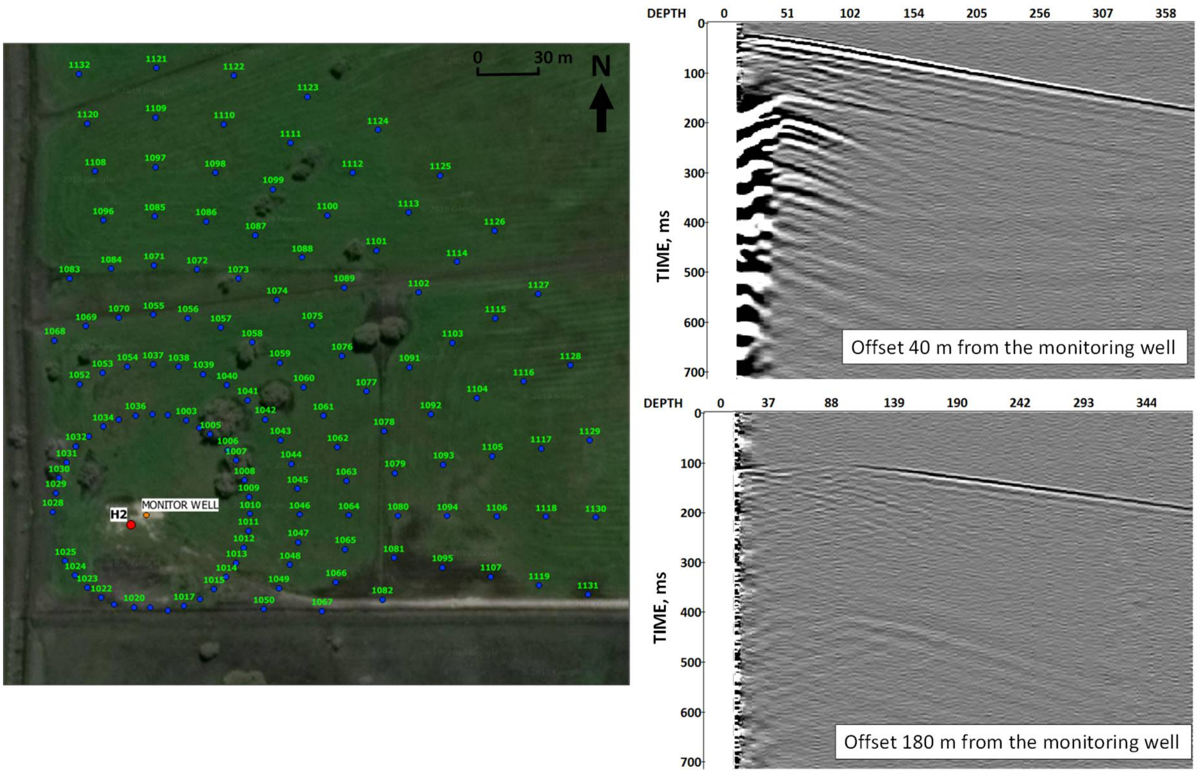

Figure 9. Left: Acquisition map of the offset VSP surveys at the In-Situ Lab research site. Blue points are the shot point locations. The red point is the Harvey-2 well and the orange point is the location of ISL OB-1. Right: DAS data from the monitoring well. Gathers (stack of 8 shots): top panel – from one of the near offsets – 40 m; bottom panel – from one of the far offsets – 180 m.

A 1.2 kJ electrical sparker in ISL OB-1 was utilised to assess the feasibility of the cross-well seismic method paired with DAS in the Harvey-2 well, and data was acquired without interrupting the injection. Cross-hole data was collected daily; the sparker was at the depth range of 60-200 m (with a step of 20 m) for each survey, emitting thirty times at every level.

Electric resistivity imaging (ERI)

Time-lapse detection of changes in electrical properties around the instrumented monitoring well was performed by intensive monitoring immediately before and during the CO_2 injection phase, followed by less frequent post injection surveys. Although a large number of configurations were modelled, data acquisition with the fast dipole-dipole electrode configuration with reciprocal measurements (770 quadrupoles) was selected for deployment. Each survey took approximately 10 minutes, permitting rapid acquisition time and acceptable data quality. Some 145,920 electrode quadrupole measurements were acquired during 135 surveys.

'SYSCAL Pro' was used to acquire data. SYSCAL Pro electrical resistivity measurement equipment was deployed to the site that accepted 72 channels (e.g. wires from 72 electrodes) via three military-standard style plugs (i.e. each plug accepting 24 channels). Connection of the 32-channel downhole electrode array to the SYSCAL Pro required design and manufacture of a "patch box". The patch box splits wiring for electrodes 1 to 24 into the first plug (channels 1-24) and a further 8 wires to channels 25 to 32 onto the second plug. The patch box was designed to facilitate on-site modification to wiring as required.

Downhole logging

Induction logs were obtained ten times in the cased ISL OB-1 well and pulsed neutron (PN) logging was obtained before and after the CO_2 injection in Harvey-2 well (above the perforation zone) and in ISL OB-1 (post-injection only down to 280 m depth). The logs were used to monitor possible time-lapse differences in water saturation.

Assurance monitoring

While deemed extreme unlikely based on the site geology, difference in water salinity between the injection interval and the surficial aquifer, and reservoir simulations, the potential for migration of CO_2 to groundwater or the atmosphere needed to be considered for regulatory compliance. Cement bond logs were run that confirmed contiguous cement fill along the wellbore. Continuous DTS monitoring as well as groundwater and soil gas sampling was performed for detecting potential CO_2 vertical migration along microchannels between the cement and the well casing or between the cement and the rock.

The air and soil monitoring activities commenced a month prior to injection and details are provided by Myers et al. (2020). Data on both the CO_2 concentration and flux was collected using a range of automated and manual approaches. The carbon dioxide concentration in the air directly above the soil surface was periodically measured around the site using a Picarro-based mobile system whereas the CO_2 concentration in the vicinity of the injection and ISL OB-1 monitoring wells were determined using permanently mounted Li-COR (Li-840A) analysers. In addition, gas sampling of the soil vadose zone was performed and samples were submitted for carbon isotope and gas composition analysis. In terms of soil flux measurements, these were made near the wells (i.e., injection, monitoring and groundwater) and at a more distant reference location using a permanent solar powered/battery system that comprises a Li-COR (Li-8100A) analyser with four semi-permanent flux chambers whereas regular soil flux surveys at gridded locations (typically 5-10 m spacing) were achieved with a West Systems portable analyser over an area of approximately 50 m x 70 m located around the monitoring well.

Three groundwater sampling campaigns took place before CO_2 injection started at Harvey 2 (between November 2018 and January 2019), three during the injection period and five after injection finished (February - March 2019). Analyses included field parameters, major and minor ion concentrations, alkalinity, dissolved CO_2 concentration, carbon isotopes, and total inorganic carbon (TIC)/total carbon (TC)/total organic carbon (TOC).

Three component seismic recorders were installed across the well site and on the nearby farmland to monitor the injection-related seismicity and any other relevant seismic activity. Each of the seismic recorders was comprised of a three component (vertical, north and east) 15 Hz seismic sensor (GS-One), a digitizer with built-in GPS receiver (Geospace GSX), and a battery unit. The sampling rate of the signals in the digitizer was set to 500 Hz with continuous recording. The GPS unit regularly received time-stamp from corresponding satellites and used this information to self-correct the electronic time drift due to the heat fluctuations. Stations were distributed to cover both the immediate injection area and far field to have an even coverage. Out of 30 stations, 9 were installed at a single point, with an approximate distance of 400 m away from the injection point; a closer location was not feasible due to existing infrastructure and disturbance by surface activities and on the well pad. These tightly clustered stations were used to increase the signal-to-noise ratio of the recorded signals in the analyses.

4. CO_2 controlled release experiment

This section describes the CO_2 injection experiment and presents some initial monitoring results and preliminary discussion, while detailed interpretation of the extensive monitoring data sets and modelling are ongoing activities to be reported in the future.

4.1 Injection operations

Injection started 5th February and concluded on 9th February with a total volume of 38 tonnes injected over 101 hours, corresponding to an average injection rate of approximately 0.4 tonnes per hour. Pressure measurements at the wellhead (WHP) and at reservoir level (BHP) in Harvey-2 were used to monitor and guide injection operations (Figure 10). The anticipated injection pressures for the experiment were modelled to be below 4000 kPa at the injection interval and an injection rate of up to 1 tonne/hour.

After an initial pressure increase associated with the flushing of the water present in the well, the WHP and BHP stabilised at around 3500 kPa and 4000 kPa, respectively (**Error! Reference source not found.**). The WHP was higher than predicted (which minimized the presence of liquid in the pumping system) indicating in a lower than desired injection rate (approximately 0.1 tonnes/hour).

The initial AGD-7 gas pump was combined with an ASF-B10 liquid pump approximately 24 hours after injection started without delivering an appreciable improvement in injection rate. Approximately 6 hours later (30 hours) this system was replaced by a larger ATV-8 liquid pump increasing injection rate initially to 0.4 tonnes/hour. However, the rate declined to 0.25 tonnes/hour due to operational problems related to the heater and pump. As a result of the initial increased injection rate, the WHP and BHP increased to 4000-4500 kPa and 5000 - 5500 kPa, respectively. No change of injection rate was observed after refilling the ISO tank (42 hours).

The BHP increased steadily until a leak in the injection line caused injection to be paused at 58 hours for 8 hours. As expected, the BHP declined while injection was stopped. During this time a needle valve connected to a redundant pressure gauge and impeding flow was removed from the wellhead. Injection recommenced at 66 hours and an approximately 0.8 tonnes/hour injection rate was achieved. Rates were reduced to 0.6 tonnes/hour to enable continuous injection prior to the second refilling of the CO_2 tank. After the refill (at 88 hr), injection rates reached 1 tonne/hour at a maximum WHP of 5500 kPa, corresponding to a maximum bottomhole pressure of approximately 6600 kPa (Figure 10).

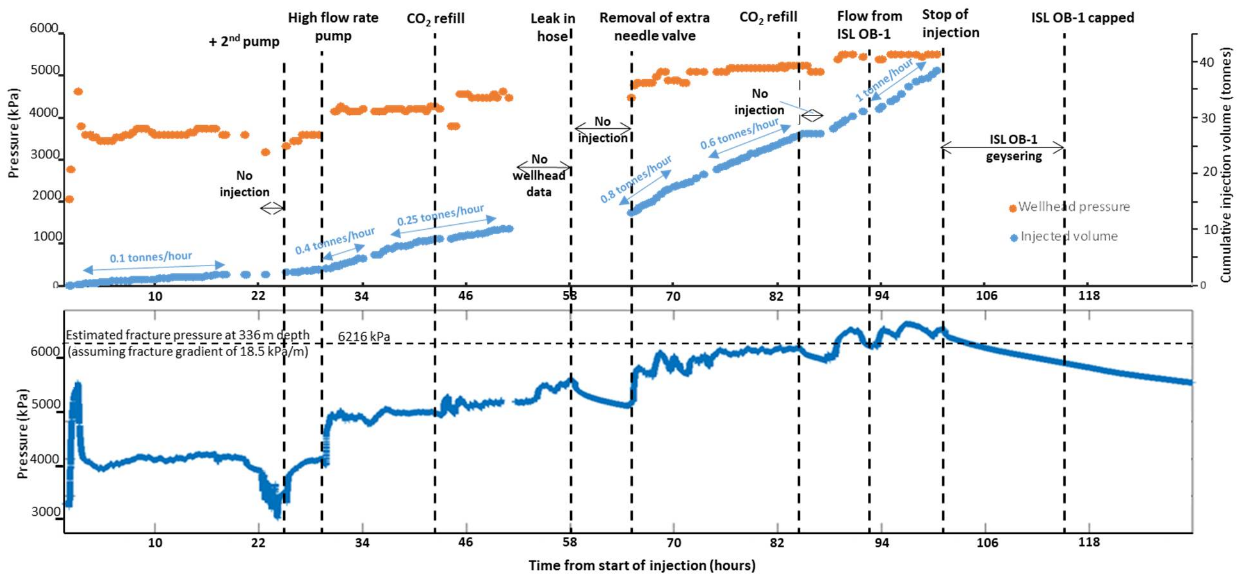

Figure 10. History of wellhead pressure, cumulative injection volume and injection rate (top), correlated with observed reservoir pressure (bottom) in Harvey-2 and with operational activities and selected incidents.

Temperatures at the wellhead ranged widely between 85 °C at low injection rates and 20 °C at high injection rates (Figure 11). Bottom hole temperature remained relatively constant during injection between 27.5 and 30 °C, slightly lower than the initial reservoir temperature of 31 °C. For these temperatures and most of the observed pressures the CO_2 exists as a vapour. However, at bottomhole pressures above 6000 kPa, CO_2 is injected close to the liquid-vapour line and observed temperature decreasing to as low as 24 °C indicates occasional two-phase conditions for short time towards the end of injection.

At 94 hours, ISL OB-1 was observed to be flowing water, BHP had exceeded 6200 kPa at that point in time. While monitoring of pressure, DTS and DAS continued, injection was stopped at 101 hours in response to an eruptive release of formation water and CO_2.

All unnecessary personnel were removed from site and the well was allowed to depressurise naturally by a total of seven eruptive releases in form of geysering that occurred over a period of 12 hours. Once the periodicity of the expulsions had been ascertained, the well was closed with a high-pressure cap 115 hours after start of injection.

The well has since been remediated and cemented back above the leakage point to a depth of 280 m. The CO_2 was back-produced from Harvey-2 to avoid corrosion of the tubing and casing, leaving largely residual and dissolved CO_2 in the formation. Continuing monitoring includes surface CO_2 flux measurements (particularly around the injection and monitoring well), groundwater sampling, reservoir pressure and temperature in the injection well (Harvey-2) and downhole measurements in ISL OB-1 using the fibre optics (DTS and DAS). There is no indication from DTS, induction or PN logging of CO_2 migration above the injection zone at 336 m depth. Six months after ceasing injection, no CO_2 concentrations above baseline have been detected in the groundwater well or at the ground surface.

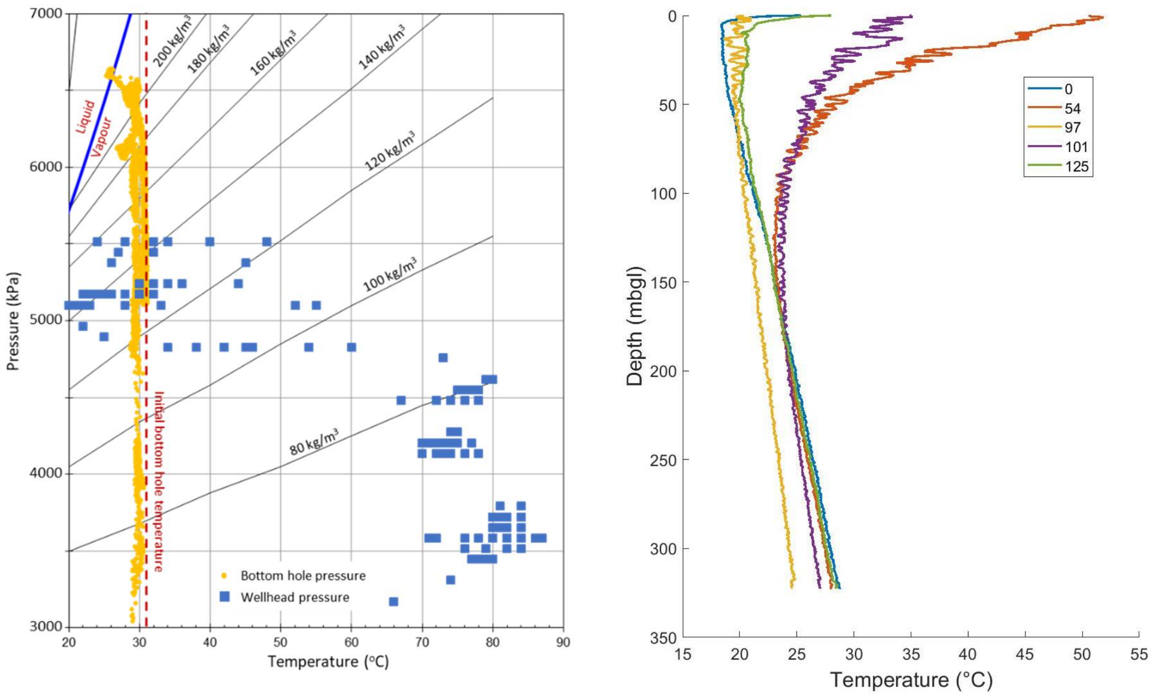

Figure 11. Variation of pressure and temperature during CO_2 injection. Left: Pressure versus temperature variations measured at the wellhead and bottom of Harvey-2 showing impact on CO_2 density (CO_2 density contours and vapour-liquid line are based on Span and Wagner, 1996). Right: DTS data along the length of Harvey-2 for various times during the controlled-release experiment. 0 hrs: start of injection, 54 hrs: during injection of hot CO_2 gas, 97 hrs: during high-rate injection of relatively cool CO_2 (< 30 °C) and liquid phase event, 101 hrs: towards the end of the experiment, and 125 hrs: one day after the end of injection.

4.2 Distributed temperature sensing (DTS)

The DTS provided very accurate, robust and detailed information about each stage of the CO_2 injection test. The installation at Harvey-2 provided insides into the temperature profile and variation of CO_2 properties in the injection well (Figure 11, right). The observed temperature changes correlate very closely to the pressure, flow rates and the heater performance. When the heater is delivering a gaseous CO_2 at high temperature, the excess temperature is dissipated in the upper section of the well (54 hrs in Figure 11, right). The temperature profile then follows a similar gradient as the baseline temperature. Occasionally, with high flow rate and heater not performing at maximum capacity, the injection temperature gradient is steeper than the baseline gradient with temperatures as low as 25 degrees at the bottom of the well (97 hrs in Figure 11, right), indicating the presence of a liquid phase at bottom hole depth. This condition is present in the well for several hours but then injection of pure gaseous CO_2 is reinstated as reflected by the temperature profile at 101 hours the end of injection. One day after injection has ceased (125 hrs in Figure 11, right), the temperatures have returned to baseline conditions for the lower 200 m of the well.

DTS in ISL OB-1 (Figure 12) allowed the identification of CO_2 arrival as well as the characterization of the in-well leakage events in both time and space. The evolution of temperature changes (expressed relative to baseline) is presented for a selection of depths from the ISL OB-1 data set (Figure 12). At 30 hours after start of injection, the first increase in temperature occurred at 335 m (immediately below the sealing paleosol) indicating the first arrival of CO_2 after approximately 5 tonnes of injection. This coincides with a sharp increase in bottom hole pressure by approximately 1000 kPa in response to the higher injection rates after replacing the pump (Figure 10). Joule-Thomson heating due to the increase in pressure in the injection interval could explain why CO_2 arriving at ISL OB-1 is warmer than at the point of injection. No temperature changes were observed above the paleosol at 331 m, indicating a lack of vertical CO_2 migration beyond the injection interval at that time.

After 54 hours, increased temperatures can be seen at 341m and 356 m and the rate of temperature began to increase between 335 and 341 m, which is interpreted as an up to 5 m thick accumulation of warm CO_2 below the paleosol. A sharp temperature increase can be observed at 88 hours at 331 m depth, corresponding to a slight drop in temperature at 341 and a decline in temperature from 356, while the temperature at 335 continued to rise steadily. This event is interpreted to coincide with CO_2 and formation water entering the well through the damaged fibreglass casing. Cooling at the top of the well (1 m depth in Figure 12) is probably due to opening of the wellhead and water flowing from the well (at 88 hours in Figure 10). The 7 expulsion events of formation water and CO_2 are reflected by cyclic temperature changes (from 100 – 115 hours) at all depths at and above the injection interval.

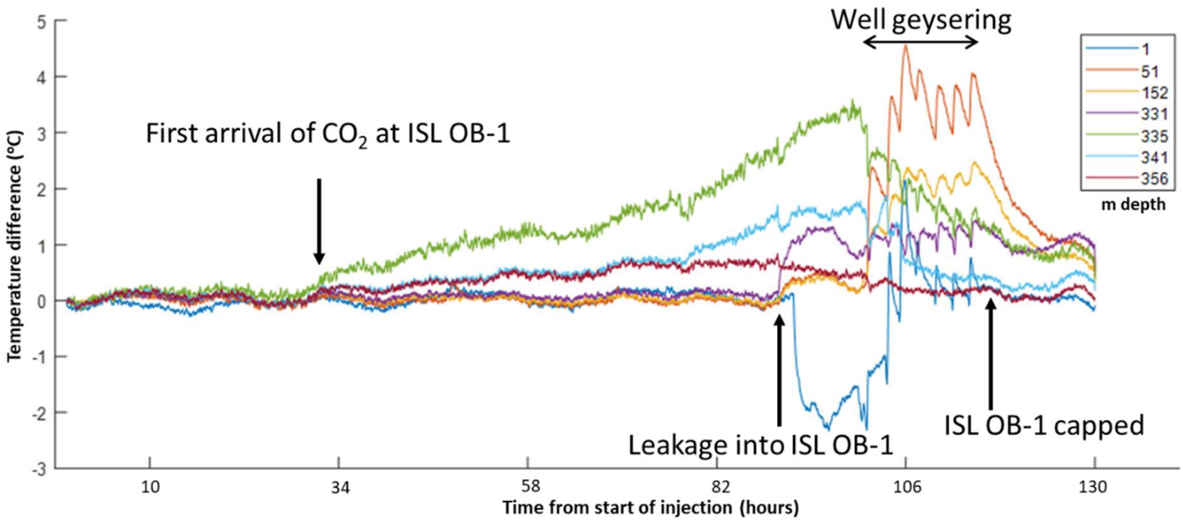

Figure 12. Temperature difference at selected depths in ISL OB-1 during and post injection from 5th February to 11th February 2019. The 1 m, 51 m and 152 m data are chosen to show the general temperature range down hole at 50 m intervals. The data gathered at 335 m is just below the paleosol interval and near the top of the perforated interval. Data for 341 m is within the perforated interval and 356 m is some 14 m below the base of the perforated interval.

The well geysering can be explained by a two-phase flow process (flashing) in which CO_2 comes out of solution as the fluid rises in the well. CO_2 solubility in water is observed to decrease with reduction in pressure and temperature as the water rises (Lu et al.,2005; Watson et al., 2014).

4.3 Borehole seismic

The pressure data, physical observations and distributed temperature data observations are supported by the borehole seismic results. Offset VSP data are of good quality and a high level of repeatability was achieved that enabled the detection of a small amount of the injected CO_2, even in anticipation of a relatively low signal. The signal to noise ratio was significantly improved by stacking the shot points located around the monitoring well at the constant nearest offset (40 m) to produce an effective zero-offset VSP geometry in a single ensemble. The reliability of the time-lapse seismic images depends on many factors: changes in the media, the fidelity of sources' and receivers' positions, and consistency of the source signature. The normalised root mean square (NRMS) parameter is a measure of consistency. The NRMS is 0 when two datasets are identical, 140 in the case of random noise, and 200 for a dataset with opposite polarity (Kragh and Christie, 2002). The NRMS estimate between the baseline and the eighth monitor dataset (after injecting 38 tonnes of CO_2) in Figure 13d are attributed to the high repeatability rate reached, even considering relatively low power seismic source used for the survey. The wavelet for deconvolution was estimated for each shot location and vintage separately. Figure 13 (a-c) shows deconvolved gathers of the baseline data, data from the eighth monitor vintage) and their difference. Data is normalised over all three sections for display purposes, and the remains of the direct on the difference section are visible but very insignificant with respect to initial amplitudes. A clear manifestation of the time-lapse signal is observed on the difference section at the target depth (highlighted by the red arrow). Slight differences in the images to baseline can be seen as early as the fourth monitor vintage at which point 7 tonnes of CO_2 had been injected after 44 hours.

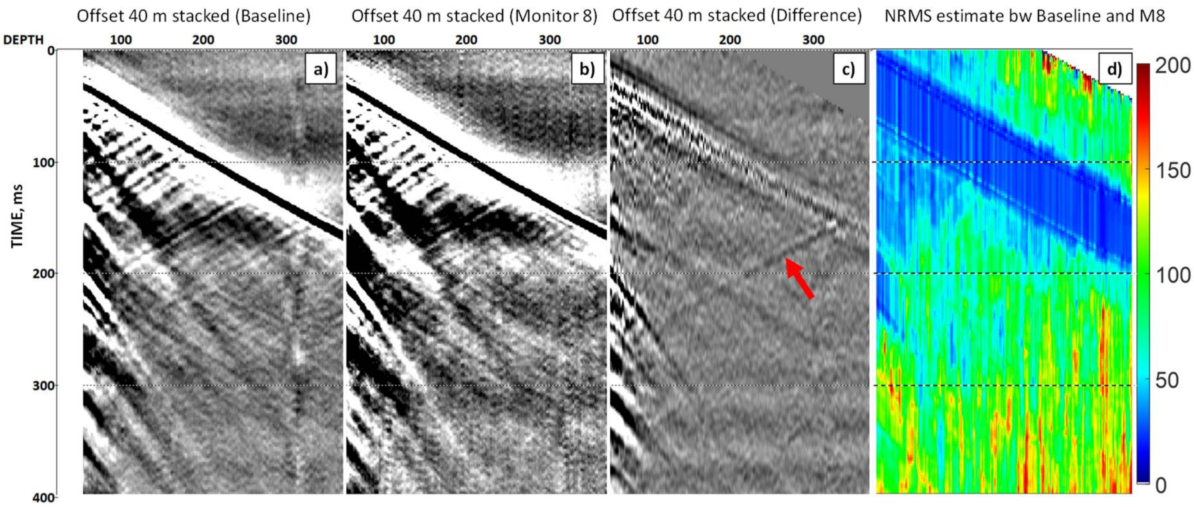

Figure 13. Time-lapse images of the CO_2 plume on VSP sections. a) baseline seismogram; b) monitor 8 seismogram; c) differences of the baseline and monitor data; d) NRMS estimate between baseline and monitor 8 datasets. Red arrow indicates clear response from the injected gas.

Due to issues related to faulty connections during the installation of the hybrid cable, the cemented geophones were not active for every survey, and as such data analysis was primarily focused on DAS data. It would be desirable to increase signal to noise ratio of the active seismic data to elevate the level of detectability that could be achieved by introduction of a more powerful source. In the future, continuous recording with the behind-casing sensors would provide significant advantages for observation of various aspects of the experiment as well as microseismic monitoring. Alternative approaches of reverse VSP for similar shallow rapidly developing processes should be discussed as it allows extremely fast acquisition of a single vintage and use of high frequency downhole sources.

Implementation of the cross-well approach suffered from operational noise caused by the injection process in Harvey-2 impacting the signal, hence the analysis of these data has been problematic. Alternatively, the cross-hole approach should be considered in a number of passive observation wells, or during breaks in the injection operations.

4.4 Electrical resistivity imaging

Excellent survey repeatability was achieved by this method and details are provided by Harris et al. (2019). Significant changes in dipole-dipole apparent resistivity were observed at the injection interval from 82 hours after the injection of 25 tonnes of CO_2, and it is possible to identify changes in apparent resistivity close to the injection depth interval (336 – 342 m). Whether these resistivity changes are due to the presence of CO_2 or flow of formation water is under investigation. It should be noted that the limitation of these results is largely due to the electrode spacing having been designed for detecting vertical migration of CO_2 over a larger thickness than observed in the experiment.

4.5 Downhole logging

Induction logs showed no changes in either deep or shallow resistivity above 345 m between the baseline log and the first six runs during the injection. The log obtained post injection shows significant change in resistivity due to the change of the environmental parameters. However, the calibrated log shows no difference with the baseline obtained prior to CO_2 injection down to the 330 m.

Pulsed neutron logs obtained in ISL OB-1 and Harvey-2 show only small changes in water saturation above the injection zone. This may be interpreted as CO_2 saturation of less than 10% at each well, however, this is unlikely as other observations do not show any sign of vertical CO_2 migration. If those changes are caused by CO_2 migration, one would expect the differences to increase over time and be more reliably detectable above the perforation zone.

4.6 Assurance monitoring

Apart from the elevated CO_2 levels which were observed for a very short period in the soil surface around the ISL OB-1 monitoring well due to the well geysering, no anomalous CO_2 has been detected up to two months post injection. The measured CO_2 soil flux and concentration four weeks post injection are within the range of baseline levels observed prior to injection. Parts of the surface monitoring program (i.e., Li-COR, West Systems, soil-gas sampling) will continue for a significant period after injection.

Based on the groundwater monitoring results, groundwater in the Superficial aquifer within the study has a salinity above 5000 mg/l and is suitable for irrigation and livestock purposes only. In contrast, formation water salinity in the CO_2 injection interval, the Eneabba Formation, is on the order of 25,000 mg/L and too high to be suitable for any use. No significant changes in the water chemistry in the In-Situ Lab groundwater well were observed during the monitoring period suggesting that injection of CO_2 into the Eneabba Formation had no impact on the Superficial aquifer.

The discharge from ISL OB-1 during geysering was initially borehole fluid (freshwater), followed by formation water (~25,000 mg/L) and CO_2 plus some minor amounts of drilling fluid and formation sand. Based on the volume of the well and CO_2 solubility, the total volume of formation water which spilled onto the limestone pad was estimated to be <20,000 L and the volume of CO_2 emitted to atmosphere less than 2 tonnes.

The relatively high levels of ambient seismic noise and low number of sensors prevented passive seismic from picking the onset of any events during the injection experiment. In the future, the number of elements of the array should be increased and augmented with three components downhole sensor deployment. The deployment of a large N type array will help the identification of the coherent energy packet with higher confidence.

5. Discussion

5.1 Fault zone structure

Stratigraphic correlations using log data from Harvey-2 and ISL OB-1 do not show any structural vertical displacement between the two wells at the depth of injection. This confirms that in this area the paleosol at the top of the injection interval is contiguous and forms a barrier to vertical CO_2 migration. Concentration of carbon dioxide within a thin interval is also confirmed by the borehole seismic as there is only a reflection like time-lapse signal observed at the injection depth, but no signal above. However, the new well and the controlled release experiment did not provide further details on fault zone geometry. Additional high resolution seismic targeting the 0-400 m depth interval is required for improving the structural interpretation of the test site.

5.2 Injectivity estimation

Based on the limited data from the short water production and injection tests prior to CO_2 injection, a productivity index (PI) for the perforation interval was estimated to be on the order of 0.01 m^3/day/kPa. This compares to a theoretical PI of 1.5-2.0 m^3/day/kPa assuming a 5 Darcy permeability and 6 m thickness of the perforated interval.

Applying the analytical method from Mathias et al. (2008,2009) confirms that a reduced permeability on the order of 30 mD is needed to explain the high bottomhole injection pressures during the controlled-release experiment. Bottomhole pressures for average rates of 0.1, 0.4, 0.6 and 0.8 tonnes/hour were estimated at 3922, 5307, 6100 and 6830 kPa, respectively for a 6 m injection interval, a constant temperature of 29 ^{o}C, an initial reservoir pressure of 3300 kPa, and a porosity of 25 %. These pressure values fall within a comparable range to the observed reservoir pressures in Figure 10 for the respective injection rates. It should be noted that this analysis assumes constant fluid and rock properties, does not account for thermodynamic effects and buoyancy, and the high compressibility of gaseous CO_2 may lead to a slight overestimation of bottomhole pressures (Mathias et al., 2009).

The reasons for the very high skin factor above 100 were assessed by investigating the drilling history of Harvey-2. Harvey-2 was initially drilled for collecting geological data including core, and the well was not planned to be used as a fluid producer or injector. The well was left uncased below 207 m for an extended period of time for logging and coring activities, and wellbore stability issues were managed by increasing mud weights to up to 1.17 SG. The resulting mud cake in the injection interval is estimated to be up to 750 mm in diameter, which is more than double the 290 mm target penetration of the perforating gun. Future experiments will require remediation of the injection interval (e.g. air lift juttering, acidization) or establishment of deeper perforations beyond the mud cake.

5.3 Pressure and temperature evolution

The understanding of the injected gaseous CO_2 has greatly benefitted from the downhole and geophysics monitoring. However, the lower than expected injectivity has created interesting well thermodynamics challenges that would need to be taken into consideration in the interpretation and the integration of the downhole dataset in view of the interpretation of CO_2 injectivity and the CO_2 plume imaging. The temperature monitoring shows that thermal effects are non-negligible and must be considered in reservoir simulations, at least close to the injector. A preliminary analysis of the pressure and temperature evolution from Harvey-2 shows that phase transition occurs in the wellbore during later stages of injection. As already pointed out when listing the limitations of the analytical reservoir calculations in the previous section, coupled non-isothermal wellbore-reservoir simulations are required to adequately model the observed pressure and temperature evolution, and the migration of CO_2 during the controlled-release experiment.

5.4 Contribution to the Shallow Release Portfolio

The test at the In-Situ Lab addressed several gaps regarding shallow-release experiments noted in Roberts and Stalker (2017), with respect to:

- Depth; the test was conducted significantly deeper than most shallow release experiments; 336 m rather than <25 m.
- Top seal; the absence of a thick regional shale in this area means that industry, regulators and public all have an interest in understanding the behaviour of a potential leak and how the top seal, in this case paleosols, might behave if CO_2 leaked, if the site becomes a future commercial-scale operation.
- Volume; 38 tonnes in this single experiment is approximately 4 times larger than for any previous site where shallow release experiments took place (Ginninderra; Roberts and Stalker, 2017 and references therein). Of the reviewed experiments, 82.8 tonnes CO_2 had been injected in total. Only the CaMI project in Canada has been injecting at comparable rates of approximately 0.4 t/day over a longer timeframe at a depth of approximately 300 m (Goodarzi et al., 2019).
- Identification of leakage; as little as 7 tonnes CO_2 was imaged at a depth of 336 m in one of the earlier seismic vintages and the 38-tonne plume was observed in the later seismic vintages. First arrival was observed within 30 hours by DTS.

One of the main issues identified in Roberts and Stalker (2017) was the leakage of CO_2 along wellbores or pipelines constructed to introduce the CO_2 or to monitor it underground. In this experiment wellbore leakage was encountered in the fibreglass cased ISL OB-1 monitoring well. DTS and DAS provide a comprehensive data set for better understanding and ongoing modelling of the thermo-hydrodynamics of flow processes inside a well, and for monitoring the remediation operations.

6. Summary and conclusions

The objectives of the In-situ Lab CO_2 controlled-release test were to assess the monitorability of shallow, gaseous CO_2 accumulations, and to investigate two-phase flow processes in a fault zone.

6.1 Monitorability of shallow gas accumulations

The test has demonstrated that DTS and downhole seismic were able to detect a plume of less than 38 tonnes of gaseous CO_2 at approximately 336 m depth. To this point, it is a qualitative observation and more work is needed for determining the lateral extend of the plume and its thickness away from the observation well. It still provides a valuable complement to the existing suite of shallow release data sets by investigating the processes associated with the accumulation of gas in the overburden above a potential commercial-scale injection site. It demonstrates the ability to monitor CO_2 accumulations previously not investigated in very near surface release experiments or deep storage test.

The detectability of the plume has been largely successful by casing-conveyed instrumentation, while wireline time lapse logging and ERT could not be adequately assessed due to limited access to or insufficient vertical resolution across the interval of interest during the test. The continuously recorded pressure and temperature data at the injection depth in Harvey-2 and DTS data from Harvey-2 and ISL OB-1 provide a comprehensive data set for detailed interpretation of CO_2 behaviour during the shallow release experiment and calibration of reservoir simulations. Coupled non-isothermal wellbore-reservoir simulations will be performed to adequately model the observed pressure and temperature evolution, and the migration of CO_2 during the controlled-release experiment.

The detectability of such a small amount compared to a commercial scale injection (i.e., 800,000 t/year over 30 years has been deemed feasible for the SW Hub; Sharma and Van Gent, 2019) is a promising achievement regarding the monitorability of potential leaks in the shallow subsurface before detection at the ground surface. However, the controlled release experiment was focussed on a relatively small area and an engineered location. More research needs to be done on improving detectability but also monitoring instrumentation for detecting more dispersed leakage, both laterally and vertically.

No anomalous CO_2 has been detected in the groundwater or the soil up to two months after the injection test. DTS data in the three wells and PN logging in ISL OB-1 have not detected any CO_2 above the injection interval, suggesting that the injected CO_2 has not migrated vertically from the injection zone in the vicinity of the wells.

6.2 Impacts of the fault zone geology

The second part of the experiment was to investigate two-phase flow processes in a fault zone. The geological data and the simulations predicted the injected CO_2 to migrate vertically through the paleosol due to the fault related disturbed nature of the sediments. However, the paleosol at the top of the injection interval proved less permeable than expected from core testing and, in contrast to the modelling predictions, the injected CO_2 did not migrate vertically.

While existing seismic and observations from Harvey-2 core show that the main fault displacement lies between approximately 400-600 m depth at the location of the controlled-release experiment, the location and configuration of smaller faults in the wider fault zone remains uncertain. Higher-resolution seismic would provide a more detailed model of the fault zone structure.

Lower than expected injectivity and lack of vertical hydraulic communication resulted in higher than expected injection pressures, temporarily rising to within the fracture pressure range. However, no fracturing events have been recorded by the deployed monitoring techniques.

6.3 Well leakage

The high injection pressures, laterally focussed migration of the injected CO_2 along the base of the paleosol, and likely weakening of the fibreglass integrity during the cement drilling, resulted in a casing leak at 336 m depth in ISL OB-1.

Although the leak in the fibreglass casing was accidental, there were no adverse environmental impacts. The resulting geysering of the well provides important information to inform the risks associated with CO_2 accumulations in the shallow subsurface environment (approximately 50 times volume increase of CO_2 between 400 m depth and the ground surface) and contains valuable insights into quantifying the volumes of CO_2 and water that may be produced in such an event.

6.4 Concluding remarks

The In-Situ Lab forms an enduring and unique research facility for further research into the monitoring and characterisation of CO_2 migration in fault zones and from the shallow groundwater environment to the ground surface. Near-term improvements to the site include well remediation activities to improve injectivity and new, high-resolution seismic for better characterisation of the fault zone geometry. Demonstration of successful monitoring technologies in such setting is important for increasing public and regulator confidence in the ability to confirm the safety of CO_2 geological storage.

Acknowledgements

The In-Situ Lab project was supported by the Australian Government through the Commonwealth Carbon Capture and Storage Research Development and Demonstration Fund CCS49360. The authors wish to acknowledge the contributions by the Western Australian Department of Mines, Industry Regulation and Safety including the Geological Survey of Western Australia. We are particularly thankful for the help and advice from Dominique Van Gent and Sandeep Sharma. The comments and suggestions by two anonymous reviewers have significantly improved the contents of our paper.

References

Backhouse, J., 2015. GSWA Harvey 2 palynology report: Backhouse Biostrat Pty Ltd, report for Geological Survey of Western Australia, Report BB490 (unpublished).

Bense, V., Gleeson, T., Loveless, S., Bour, O., Scibek, J., 2013. Fault zone hydrogeology. Earth-Science Reviews, 127: 171-192.

Birkholzer, J., Cihan, A., Bandilla, K., 2014. A tiered area-of-review framework for geologic carbon sequestration. Greenhouse Gases: Science and Technology, 4: 20-35

Bourdet, J., Sarout, J., Strand, J., Delle Piane, C., Vialle, S., Langhi, L., Harris, B., Lebedev, M., Teo, B., Esteban, L., Godel, B., Dautriat, J., Emelyanova, I., Pervukhina, M., Glubokovskikh, S., Noble, R., Saeedi, A.,2019. Assessment of multi-barrier systems for CO_2 containment in the Yalgorup Member of the Lesueur Sandstone, South West Hub. CSIRO report EP19286. CSIRO, Australia.

Bradshaw, B.E., Rollet, N., Totterdell, J.M., Borissova, I., 2003. A revised structural framework for frontier basins on the southern and southwestern Australian continental margin. Geoscience Australia Record 2003/03.

Byrne, C., 2016. Seismic interpretation of the Harvey area: ODIN Reservoir Consultants Consultants Pty Ltd, report for Department of Mines, Industry Regulation and Safety, DMP/2016/1 (unpublished).

Childs, C., Manzocchi, T.,Walsh, J.J., Bonson, C.G., Nicol, A., Schöpfer, M.P., 2009. A geometric model of fault zone and fault rock thickness variations. J. Struct. Geol. 31: 117-127.

Crostella, A., Backhouse, J., 2000. Geology and petroleum exploration of the central and southern Perth Basin, Western Australia. Western Australia Geological Survey, Report 57: 75p.

Delle Piane, C., Olierook, H.K.H., Timms, N.E., Saeedi, A., Esteban, L., Rezaee, R., Mikhaltsevitch, V., Lebedev, Maxim., 2013. Facies-based rock properties distribution along the Harvey 1 stratigraphic well. CSIRO Report Number EP133710.

Feitz, A., Radke, B., Hossain, M. S., Harris, B., Schaa, R., Pethick, A., Ziramov, S., Urosevic, M., Tenthorey, E., Pan, Z., Ennis-King, J., Wang, L., Gunning, M.-E., Lai, E., Ransley, T.,Tan, K.P., Schacht, U., Kalinowski, A., Black, J.R,. and Pevzner, R., 2018. The CO2CRC Otway Shallow CO_2 Controlled Release Experiment: Geological Model and CO_2 Migration Simulations. 14th Greenhouse Gas Control Technologies Conference Melbourne 21-26 October 2018 (GHGT-14). SSRN: https://ssrn.com/abstract=3365843

Fulljames, J.R., Zijerveld, J.J., Franssen, R.C.M.W., 1997. Fault seal processes: systematic analysis of fault seals over geological and production time scales. In: Society, N.P. (Ed.), Hydrocarbon Seals

— Importance for Exploration and Production. Vol. 9 of NPF, Special Publication. Norwegian Petroleum Society, Oslo: 51–59.

Goodarzi, S., Lawton, D., Osadetz, K., 2019. Coupled fluid flow modeling in the wellbore and reservoir for CO_2 injection at the CaMI field research station, Proceedings of the 4th World Congress on Momentum, Heat and Mass Transfer (MHMT'19), Rome, Italy – April, 2019, Paper No. ENFHT 141.

Guglielmi, Y., Cappa, F., Avouac, J.-P., Henry, P., Elsworth, D., 2015. Seismicity triggered by fluid injection–induced aseismic slip. Science, 348(6240): 1224.

Harris, B., Costall, A., Nguyen, H., Michael, K., Ricard, L., Freifeld, B., Avijegon, A., Pethick, A., 2019. Time lapse in-hole electrical resistivity surveying during a shallow release of CO_2 gas: Harvey, Western Australia. Australasian Exploration Geoscience Conference; 2-5 September 2019; Perth, Western Australia: 5 p.

IPCC, 2005. IPCC special report on carbon dioxide capture and storage. prepared by Working Group III of the Intergovernmental Panel on Climate Change. Cambridge University Press, Cambridge and New York: 442 p.

Jenkins, C., Chadwick, A., Hovorka, S.D., 2015. The state of the art in monitoring and verification—Ten years on. International Journal of Greenhouse Gas Control, 40: 312-349.

Kaldi, J.G., Daniel, R., Tenthorey, E., Michael, K., Schacht, U., Nicol, A., Underschultz, J., Backe, G., 2013. Containment of CO_2 in CCS: Role of caprocks and faults. Energy Procedia, 37: 5403-5410.

King, R.C., Hillis, R.R., Reynolds, S.D., 2008. In situ stresses and natural fractures in the Northern Perth Basin, Australia. Australian Journal of Earth Sciences, 55(5): 685-701.

Kragh, E. and Christie, P., 2002. Seismic repeatability, normalized RMS, and predictability. The Leading Edge, 21(7): 640-647.

Langhi, L., Ciftci, B., Strand, J., 2013. Fault seal first-order analysis – SW Hub. Report to ANLEC R&D 7-1111-0201; http://www.anlecrd.com.au/

Lewicki, J.L., Birkholzer, J., Tsang, C.-F., 2007. Natural and industrial analogues for leakage of CO2 from storage reservoirs: identification of features, events, and processes and lessons learned. Environ. Geol., 52(3): 457-467.

Lim, D., Strachan G., van Gent D., Sharma S., 2017. Underground storage of carbon dioxide in the Harvey area, south-west Western Australia. The APPEA Journal, 57: 177–210.

Low, G.H., 1971. Definition of two Quaternary formations in the Perth Basin., Geological Survey of Western Australia. Annual Report, 1970: 33-34.

Lu, X., Watson, A., Gorin, A.V., Deans, J., 2005. Measurements in a low temperature CO_2-driven geysering well, viewed in relation to natural geysers. Geothermics, 34(4): 389-410.

Macquet, M. and Lawton, D.C., 2019. Exploring continuous seismic data for monitoring CO_2 injection at the CaMI Field Research Station, Alberta, Canada, SEG International Exposition and Annual Meeting. Society of Exploration Geophysicists, San Antonio, Texas, USA: 5p.

Mathias, S., Hardisty, P., Trudell, M., Zimmerman, R., 2008. Approximate solutions for pressure buildup during CO_2 injection in brine aquifers. Transport in Porous Media, 79(2): 265-284.

Mathias, S.A., Hardisty, P.E., Trudell, M.R., Zimmerman, R.W., 2009. Screening and selection of sites for CO_2 sequestration based on pressure buildup. International Journal of Greenhouse Gas Control, 3(5): 577-585.

Michael, K., Golab, A., Shulakova, V., Ennis-King, J., Allinson, G., Sharma, S., Aiken, T., 2010. Geological storage of CO_2 in saline aquifers - A review of the experience from existing storage operations. International Journal of Greenhouse Gas Control, 4(4): 659-667.

Michael, K., Whittaker, S., Varma, S., Bekele, E., Langhi, L., Hodgkinson, J., Harris, B., 2016. Framework for the assessment of Interaction between CO_2 geological storage and other sedimentary basin resources. Environmental Science: Processes & Impacts, 18: 164-175.

Myers, M., White, C., Pejcic, B., Feitz, A., Roberts, J., Oh, Y.-Y., Xu, L., Ricard, L., Michael, K., Avijegon, A., Rachakonda, P. K., Woltering, M., Larcher, A., Stalker, L., and Hortle, A., 2020. CSIRO In-Situ Lab: A multi-pronged approach to surface gas and groundwater monitoring at geological CO_2 storage sites. Chemical Geology, 545: 119642.

Miocic, J.M., Gilfillan, S.M.V., Roberts, J.J., Edlmann, K., McDermott, C.I., Haszeldine, R.S., 2016. Controls on CO_2 storage security in natural reservoirs and implications for CO_2 storage site selection. International Journal of Greenhouse Gas Control, 51: 118-125.

Mory, A.J., 1995. Geology of the Wedge Island 1:100 000 Sheet, Geological Survey of Western Australia. Explanatory Notes, 1v: 19p.

Olierook, H.K.H., Delle Piane, C., Timms, N.E., Esteban, L., Rezaee, R., Mory, A.J., Hancock, L., 2014. Facies-based rock properties characterization for CO_2 sequestration: GSWA Harvey 1 well, Western Australia. Marine and Petroleum Geology, 50: 83-102.

Playford, P.E., Cockbain, A.E., Low, G.H., 1976. Geology of the Perth Basin, Western Australia., Geological Survey of Western Australia. Bulletin, 124.

Pevzner, R., M., Urosevic, and S., Nakanishi, 2010. Applicability of zero-offset and offset VSP for time-lapse monitoring–CO2CRC Otway project case study: In 72nd EAGE Conference and Exhibition incorporating SPE EUROPEC 2010.

Roberts, J.J and Stalker, L., 2017. What have We Learned about CO_2 Leakage from Field Injection Tests? Energy Procedia, 114: 5711-5731.

Roberts, J.J., Wood, R.A., Wilkinson, M., Haszeldine, S., 2015. Surface controls on the characteristics of natural CO_2 seeps: implications for engineered CO_2 stores. Geofluids, 15(3): 453-463.

Roberts, J.J., Stalker, L., Shipton, Z.K., Burnside, N., 2018. What have we learnt about CO_2 leakage in the context of commercial-scale CCS? 14th Greenhouse Gas Control Technologies Conference Melbourne 21-26 October 2018 (GHGT-14), SSRN: https://ssrn.com/abstract=3366113.

Roberts, J.J., Leplastrier, A., Feitz, A.J., Shipton, Z.K., Bell, A.F., Karolytė, R., 2019. Structural controls on the location and distribution of CO_2 emission at a natural CO_2 spring in Daylesford, Australia. International Journal of Greenhouse Gas Control, 84: 36-46.

Rockwater Pty Ltd, 2015. Detailed lithological log, Southwest Hub geosequestration, Harvey 2.

Roestenburg, J., 2016. The interpretation of image data for depositional facies orientation used in building a Static Model for the Harvey CO_2 sequestration area. ODIN Reservoir Consultants - DMP/2016/2.

Sharma, S., Van Gent, D., 2019, The Australian South West Hub Project: Developing confidence in migration assisted trapping in a saline aquifer – understanding uncertainty boundaries through scenarios that stress the models. 14th Greenhouse Gas Control Technologies Conference Melbourne 21-26 October 2018 (GHGT-14). SSRN: https://ssrn.com/abstract=3366170.

Span, R., Wagner, W., 1996. A new equation of state for carbon dioxide covering the fluid region from the triple-point temperature to 1100 K at pressures up to 800 MPa. J. Phys. Chem. Ref. Data, 25(6): 1509-1596.

Sperrevik, S., Gillespie, P.A., Fisher, Q.J., Halvorsen, T., Knipe, R.J., 2002. Empirical estimation of fault rock properties. In: Koestler, A.G., Hunsdale, R. (Eds.), Hydrocarbon Seal Quantification. Vol. 11 of NPF, Special publication. Elsevier B. V., Amsterdam: 109–125.

Stalker, L., Varma, S., Van Gent, D., Haworth, J., Sharma, S. 2013. South West Hub: a carbon capture and storage project. Australian Journal of Earth Sciences, 60 (1): 45-58.

Stalker, L., and Van Gent, D., 2018. South West Hub CCS Project Research Outcomes 2017. Report to ANLEC R&D Project 7-0314-0225 South West Hub Stage 1 Integration February 2018, 56p.

Stalker, L., Van Gent, D., and NGL Project Team, 2014. South West Hub CCS Project in Western Australia – Characterisation of a Greenfield Site. Energy Procedia, 63: 5041 – 5050.

Stelfox, L., 2017. DMP Harvey 2, 3 and 4 - Well completion and preliminary observation report, Southern Perth Basin, Western Australian Department of Mines, Industry Regulation and Safety, 178 p. (available online www.dmirs.wa.gov.au/publications).

Tertyshnikov, K., R., Pevzner, M., Urosevic, A., Greenwood, and D., Popik, 2017. Offset VSP for Monitoring of the Injection of Small Quantities of CO_2–CO2CRC Otway Case Study: In 79th EAGE Conference and Exhibition 2017.

Tertyshnikov, K., H., Al Nasser, R., Pevzner, M., Urosevic, and A., Greenwood, 2018. 3D VSP for Monitoring of the Injection of Small Quantities of CO2–CO2CRC Otway Case Study: In 80th EAGE Conference and Exhibition 2018.

Timms, N., Corbel, C., Olierook, H., Wilkes, P., Delle Piane, C., Sheldon, H., Alix, R., Horowitz, F., Wilson, M., Evans, K., Griffiths, C., Stütenbecker, L., Israni, S., Hamilton, J., Esteban, L., Cope, P., Evans, C., Pimienta, L., Dyt, C., Huang, X., Hopkins, J., and Champion, D., 2012. Perth Basin Geomodel. Final Report of Project 2, Perth Basin Assessments Program, WAGCoE Report EP122443.

Timms, N. E., Olierook, H., Wilson, M., Delle Piane, C., Hamilton, P.J., Cope, P. and Stütenbecker, P., 2015. Sedimentary facies analysis, mineralogy and diagenesis of the Mesozoic aquifers of the central Perth Basin, Western Australia. Marine and Petroleum Geology, 60: 54-78.

Watson, Z.T., Han, W.S., Keating, E.H., Jung, N.-H., Lu, M., 2014. Eruption dynamics of CO_2-driven cold-water geysers: Crystal, Tenmile geysers in Utah and Chimayó geyser in New Mexico. Earth and Planetary Science Letters, 408: 272-284.